Flight System Options for a Long-Duration Mars Airplane

Reuben R. Rohrschneider,[*] John R. Olds, [†] Robert D. Braun[†] and Virgil Hutchinson, Jr.[*]
Georgia Institute of Technology, Atlanta, GA, 30332-0150

Christopher A. Kuhl[‡]
NASA Langley Research Center, Hampton, VA, 23681

and

Stephen R. Steffes[§]
The Charles Stark Draper Laboratory, Inc., Cambridge, MA, 02139

The goal of this study was to explore the flight system options for the design of a long endurance Mars airplane mission. The mission model was built in the design framework ModelCenter and a combination of a hybrid and user-driven fixed point iteration optimization method was used to determine the maximum endurance solution of each configuration. Five different propulsion systems were examined: a bipropellant rocket, a battery powered propeller, a direct methanol fuel cell powered propeller, and beamed solar and microwave powered propeller systems. Five airplane configurations were also studied. The best configuration has a straight wing with two vertical tails. The direct methanol fuel cell proved to be the best onboard power system for a long endurance airplane and the solar beamed power system showed potential for indefinite flight. The combination of the best configuration and the methanol fuel cell resulted in an airplane capable of cruising for 17.8 hours on Mars.

Nomenclature

ARES	=	Aerial Regional-Scale Environmental Survey
C_3	=	hyperbolic excess velocity, km^2/s^2
DC	=	direct current
DMFC	=	direct methanol fuel cell
D_{pullup}	=	distance the airplane drops vertically while performing the pull-up maneuver, m
DSM	=	design structure matrix
FPI	=	fixed point iteration
gdalt	=	geodetic altitude above Mars, m
IPREP	=	Interplanetary Preprocessor
LCC	=	life cycle cost, $M FY04
LV	=	launch vehicle
MMH	=	mono-methyl hydrazine
n	=	load factor
NASA	=	National Aeronautics and Space Administration
NTO	=	nitrogen tetroxide
OBD	=	optimizer based decomposition
POST	=	Program to Optimize Simulated Trajectories
SQP	=	sequential quadratic programming
W_{folded}	=	folded width of the airplane, m

[*] Graduate Research Assistant, Aerospace Engineering, 270 Ferst Dr., AIAA Student Member.
[†] Associate Professor, Aerospace Engineering, 270 Ferst Dr., AIAA Associate Fellow.
[‡] Aerospace Engineer, Exploration Engineering Branch, Mail Stop 472, AIAA Member.
[§] Guidance and Navigation Analyst, Guidance and Navigation Division, 555 Technology, AIAA Student Member.

V_{cruise} = airplane cruise velocity, m/s
Vol_{subs} = volume of airplane subsystems, m^3
Vol_{fuse} = volume of airplane fuselage, m^3

I. Introduction

THE scientific utility of Mars aerial platforms for visual imaging, spectroscopy, paleomagnetics, radar sounding, and atmospheric measurements has been identified by several authors[1,2,3]. The airplane's ability to obtain high resolution data and cover regional-scale distances gives it an advantage over orbiters and landers. To fulfill the science mission the correct suite of instruments must be carried. For this study, the ARES payload[4] will be adopted since a large amount of research has already been invested in this area. Table 1 shows the instruments carried and their payload requirements. The basic mission profile consists of launch directly into Mars transfer orbit, interplanetary cruise, direct entry at Mars, mid-air airplane deployment (pull-up maneuver), and airplane cruise. The cruise segment is performed at constant altitude from the time the airplane reaches level flight until the propellant runs out. The small time spent coasting to the ground at the end of the flight is not included. A diagram of the mission profile is shown in Figure 1.

Table 1. Science payload carried by ARES.

Instrument	Mass, kg	Power, W	Volume, cm^3
Magnetometer	1.15	0.6	635
Mass Spectrometer	4.74	6.4	3359
Point Spectrometer	3.54	16.0	24355
Context Camera	0.50	2.0	756
Video Camera	0.20	5.0	504
Totals	**10.13**	**30**	**29609 = 0.0296 m^3**

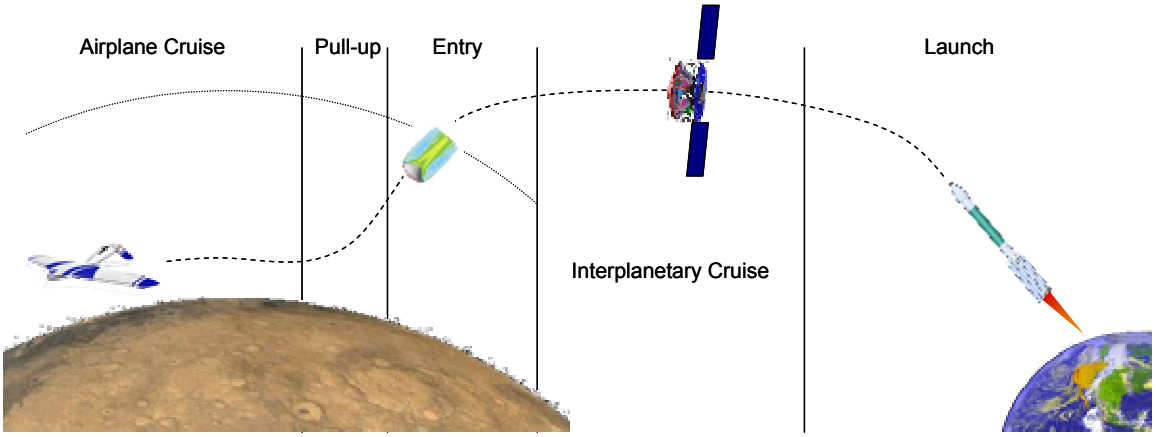

Figure 1. The Mars airplane mission profile. The science mission is performed during the cruise phase.

The goal of the science mission is to obtain as many new measurements as possible during the flight. This can be achieved by either extending the range or endurance of the airplane, or by keeping the range and endurance fixed while increasing the payload. This study will focus on increasing the airplane endurance so that more data can be gathered. Endurance improvements can be made in two ways: by changing the technologies used or by finding a combination of the design variables that produce a better solution. This study explores both of these options. First, an optimum solution will be sought for the baseline vehicle and the influence of vehicle size on endurance will be explored. The baseline vehicle will then be improved by applying different technologies and subsystems. For each technology investigated, a vehicle size study will be performed. This method ensures that all technologies are compared at their greatest potential for the given mission.

II. Model Description

The Mars airplane mission model consists of many different analyses that are broken down according to traditional disciplines. Figure 2 shows the contributing analyses assembled in a design structure matrix (DSM) for the full mission and a detail of the airplane model. In a DSM, the analysis proceeds from the upper left to the lower right with data flow indicated by a circle at the intersection of lines connecting any two analyses. Strong links are indicated by solid circles and weak links by open circles. Connections between the contributing analyses above the diagonal indicate forward flow of information, and lines below the diagonal indicate backward flow of information. A diagonal line across the analysis box indicates that the analysis includes a built-in optimizer, and grey input boxes indicate variables controlled by the optimizer. From this depiction of the model, the necessary feedback loops are easily visible, and it can be seen that changing the order of the analyses cannot eliminate the feedback loops for this problem.

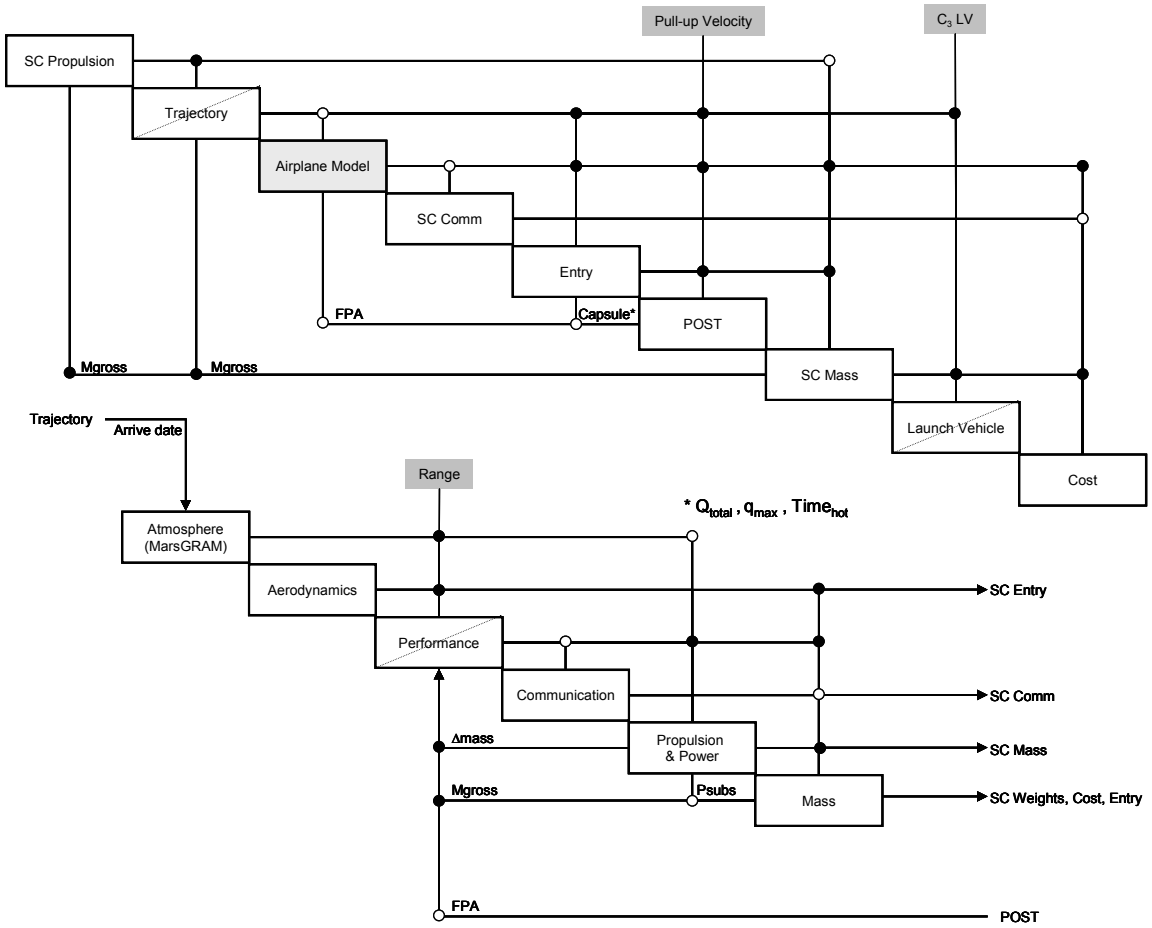

Figure 2. The Mars airplane mission analysis depicted in a DSM. The feedback links are shown and the feedback variables are labeled. Design variables controlled by the system level optimizer are shown in grey boxes.

Solving problems with feedback loops requires a scheme that ensures consistency of the feedback variables. The most common method used is fixed point iteration (FPI), but other methods also exist, such as optimizer based decomposition (OBD). These methods require running each analysis repeatedly, which is time consuming and tedious if done by hand. In this analysis, ModelCenter®, a commercially available computational framework from Phoenix Integration, is employed. Figure 3 shows the Mars airplane mission model implemented in ModelCenter using FPI to converge the model and a generic optimizer to maximize airplane endurance.

The Mars airplane mission model consists of 14 contributing analyses. To familiarize the reader with the assumptions and limitations of the model, the method behind each contributing analysis will be described.

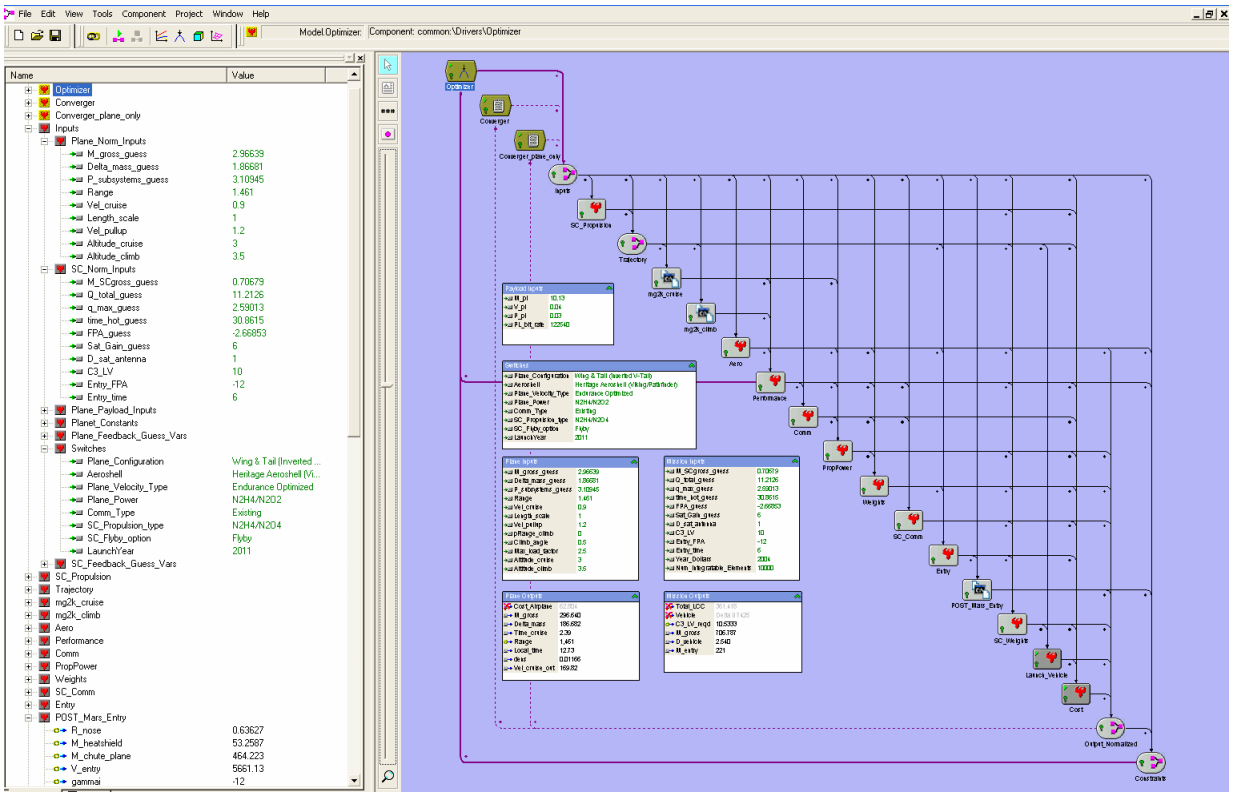

Figure 3. The Mars airplane model implemented in ModelCenter. Design variables are on the left, and a schematic of the model is in the main window.

A. Spacecraft Propulsion

The spacecraft propulsion system model sizes the main engine for the cruise stage. MMH/NTO bipropellant and MMH monopropellant rocket engines are sized using thrust required and a curve fit of rocket engine thrust to weight and dimensions[6]. Required thrust is determined by assuming a spacecraft thrust to weight of 1/10 so that instantaneous velocity changes can be assumed. The engine specific impulse, mass, and volume are output for use in the spacecraft mass analysis.

B. Interplanetary Trajectory

The trajectory from Earth to Mars was calculated using IPREP[7], a three dimensional patched conic method. IPREP was used to find the best two week launch window for each launch opportunity from 2005 until 2016. Outputs include arrival date at Mars, departure excess velocity, arrival excess velocity, required departure C_3, time of flight, and mass ratio required for the spacecraft to provide the required velocity change on departure and arrival. The departure mass ratio takes into account the C_3 capability of the launch vehicle. The final analysis consists of a table lookup which produces the required output data for each available launch opportunity.

C. Mars Atmosphere

The Mars atmosphere is modeled with Mars Global Reference Atmospheric Model 2000 to calculate the atmospheric conditions at the cruise and maximum climb altitudes for the airplane[8]. The model is used at its most basic level and requires knowledge of only the arrival date, time, altitude, and location on Mars. Altitude is measured from the Mars reference ellipsoid, and no wave model is used. The dust optical density is set to 0.3, indicating a constant low dust level, consistent with current Mars mission standards.

D. Aerodynamics & Configuration

The aerodynamics and configuration model uses photographic scaling to resize the vehicle, which allows for simple scaling of the geometry and fixed aerodynamic coefficients. Aircraft aerodynamic and configuration data is taken from previous studies where available. The baseline configuration is based on the ARES[9] study performed at NASA Langley Research Center.

Four additional configurations are also considered in this study: a straight wing with a single vertical tail[10], a straight wing with two vertical tails[11], a wing–canard[12], and a swept wing with a single vertical tail[12]. All of these aircraft originated from Earth-based flight tests with eventual interest in flight on Mars. For the configuration studies, the aircraft are folded once for each half of the wing and once for the tail. The scale size is then adjusted so that the aircraft fit into the same size aeroshell as ARES with a scale size of 1 (2.54m diameter). Figure 4 shows three of the configurations used.

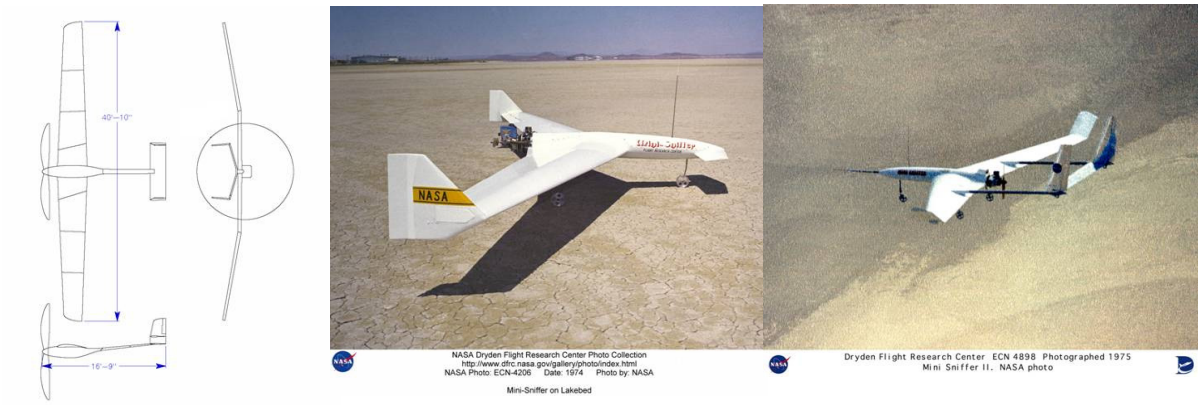

Figure 4. Three of the configurations explored in this study: Left, wing and 2 tails design; center, wing and canard design; right, swept wing and 2 tails design.

E. Airplane Performance

The aerodynamic coefficients are fed into the performance model where the range and endurance of the airplane are calculated. The performance module is also capable of calculating the cruise velocity for maximum endurance or maximum range, or simply taking a user input value[13]. The type of aircraft propulsion system determines the correct equation to use when calculating the optimum cruise velocity. The altitude lost during the pull-up maneuver is calculated using the deployment flight path angle from the entry trajectory analysis and performing a constant acceleration pull-up maneuver until the airplane reaches level flight.

F. Airplane Communication

The communication analysis computes the power and total energy consumption of the airplane transponder required to transmit the data from the airplane to a relay satellite. The relay satellite can be an existing asset in orbit such as Mars Global Surveyor, the cruise stage inserted into an Aerostationary orbit or a low Mars orbit, or the cruise stage as it flies by Mars. The last of these communication options is only feasible for short duration flights since a line of sight between the cruise stage and airplane exists for a short time period.

G. Airplane Propulsion & Power

This analysis provides five different choices of propulsion system: an NTO/MMH bipropellant rocket, a battery powered propeller, a DMFC powered propeller, a beamed solar powered propeller, and a beamed microwave powered propeller. All of the electric systems share the available power between the subsystems and the primary propulsion system while the rocket propulsion system uses primary batteries to supply electric power to the subsystems.

The bipropellant rocket system consists of a pressure fed thruster, two propellant tanks, a pressurant tank, feed lines and valves, and primary batteries. Rocket engine mass is based on a curve fit of in-space rocket engines with a thrust range from 4 Newtons to 111 Newtons. The batteries used are the same as the Li/MnO_2 batteries used for the battery powered airplane. Propellant mass is computed using the definition of specific impulse and the time of flight.

The remaining propulsion systems are propeller based. These systems share a common propeller efficiency and maximum tip Mach number of 0.85. After the propeller reaches the tip speed limit, an additional propeller is added and the diameter is decreased. The electric motor mass is based on a curve fit of small electric motors with power outputs from 2.3 kW to 11.3 kW. Gearbox mass is added to reduce the rotation rate of the propeller by a factor of two.

The battery system is computed using the energy density of the Li/MnO_2 high discharge rate batteries and the total energy required for the flight. The batteries are packaged assuming cylindrical cells with an additional 10% packaging efficiency loss.

The DMFC system is sized by calculating the cell stack mass based on the power required and the propellant mass based on the total energy required. The fuel cell stack is based on numbers published by Ballard Power Systems[14], and the combustion efficiency is based on experimental systems at Los Alamos National Labs[15,16]. The stack has a power density of 500 kW/m^3 and an efficiency of 37%.

Both of the beamed power systems calculate a beam power flux density required based on the power required for cruising flight. The airplane then carries the required power conversion system: solar cells or microwave rectennas. The hardware required on the satellite end is calculated in the spacecraft mass analysis.

The solar beamed power system uses an inflatable concentrator on the cruise stage capable of steering to track the airplane on the surface. The inflatable concentrator saves significant mass over a rigid deployable antenna[17], but introduces a dynamics problem due to the flexibility of the structure. The airplane carries solar cells on the wings, tail, and fuselage to convert the concentrated beam of light into electricity at 20% efficiency. Batteries are carried to handle 10% of the flight with a maximum of three hours. Precision tracking of the airplane from orbit is an enabling technology for this propulsion system.

The microwave power system uses a nuclear power source on the cruise stage and a microwave antenna. The antenna operates at 2.45 GHz with a DC to microwave conversion efficiency of 20%. For microwave systems the beam spread is inversely proportional to the antenna diameter, so a large antenna diameter is required to keep the total power requirement low. The rectennas mounted on the wings, tail, and fuselage convert the microwave power back to DC at 86% efficiency. The microwave antenna and rectenna are both heavier than their counterparts in the solar powered system.

H. Airplane Mass

The airplane mass analysis sums the masses of the other subsystems and calculates the mass of the vehicle structure. Parametric mass estimating relationships for unmanned vehicles[18,19] and light-weight aircraft[20] are used to estimate the structure mass. Adjustments are made where necessary to account for the difference in gravity. Outputs include the gross mass of the airplane and the power and energy required by subsystems other than communication, propulsion, and the payload.

I. Spacecraft Communication

The spacecraft communication analysis calculates the power and energy required to relay housekeeping, engineering, and science data back to Earth. The analysis assumes one eight hour window per day to communicate with the deep space network using x-band, and then calculates the required data rate based on the payload data rate and the total flight time. When the cruise stage is not used to relay science data back to Earth, the data rate is set at a low level to handle housekeeping and engineering data only. The cruise stage side of the UHF communication link to the airplane is also analyzed for power, mass, and volume requirements.

J. Entry System

The entry system scales the geometry of a 70° sphere-cone or a loaf shaped capsule[21], and estimates the mass of the complete entry system. Data from the entry trajectory is used to calculate the required thickness of the SLA-561V heat shield, taking into account both ablation and internal temperature limits. The size of the capsule is determined from the folded dimensions of the airplane with ten centimeters added in the radial direction, for clearance. The resulting aeroshell mass and outer dimensions are used in launch vehicle selection and entry trajectory calculation.

K. Entry Trajectory (POST)

The entry trajectory is calculated starting at an altitude of 125 kilometers. The initial velocity is determined using two body orbital mechanics from the conditions at the sphere of influence obtained from IPREP. The entry flight path angle is a user input since this value can be changed using small trajectory correction maneuvers. From the atmospheric interface conditions, POST[22] is used to propagate the entry capsule trajectory. Parachute deployment occurs at Mach 2, and the heatshield and airplane are deployed at subsequent user specified velocities. Outputs include the airplane deployment altitude, the maximum heat rate, the total heat load, and the time from simulation start until the airplane is deployed. This analysis primarily supports the heat shield calculations, but also ensures that the airplane deploys with sufficient clearance above the ground.

L. Spacecraft Mass

The spacecraft mass model uses fixed masses for the avionics, guidance and navigation, and sensors, and parametric models for the power systems, structure, and propulsion system. The propulsion system is sized based on the required velocity changes for both large and small maneuvers. Main engines are only included if a single burn requires a velocity change greater than 500 m/s. Nuclear electric and solar power options are included along with an option for orbit insertion of the cruise stage at Mars. If orbit insertion is not chosen, the cruise stage will enter the planetary atmosphere. The spacecraft layout is similar to that used for the ARES and Genesis missions, packaged such that the diameter of the aeroshell is the limiting dimension when configured for launch.

M. Launch Vehicle

The launch vehicle analysis uses the maximum packaged diameter, the spacecraft gross mass, and the required C_3 to select the cheapest launch vehicle capable of performing the mission. The mass and size of the spacecraft provided do not include any contingency, so the launch vehicle is selected based on the current best estimate mass. The launch vehicle database only includes vehicles from the Atlas and Delta families.

N. Cost

The cost model used is a spreadsheet implementation of the NASA Jet Propulsion Laboratory cost model[23]. These cost estimating relationships are derived from previous planetary spacecraft and provide a good estimate for the cruise stage. The model calculates the life cycle cost for the mission including phases A thru E of the project and includes a 20% reserve on phases A thru D.

Cost numbers are presented in millions of dollars in fiscal year 2004.

III. Airplane Description

The baseline vehicle for this study is based on the ARES study performed at NASA Langley Research Center[24]. The airplane is configured with a swept wing and inverted v-tail. Figure 5 shows the ARES vehicle in the flight configuration. The baseline vehicle has a wingspan of 6.26 m and a planform area of 7 m^2. Propulsion is provided by a throttled MMH/NTO rocket engine with a specific impulse of 290 s. Electrical power for subsystems is provided by Li/MnO_2 batteries. The communication system uses existing satellites to relay science data back to Earth and the airplane is deployed at subsonic speed during parachute descent of the entry system. A direct entry trajectory with a Viking-like entry capsule is employed.

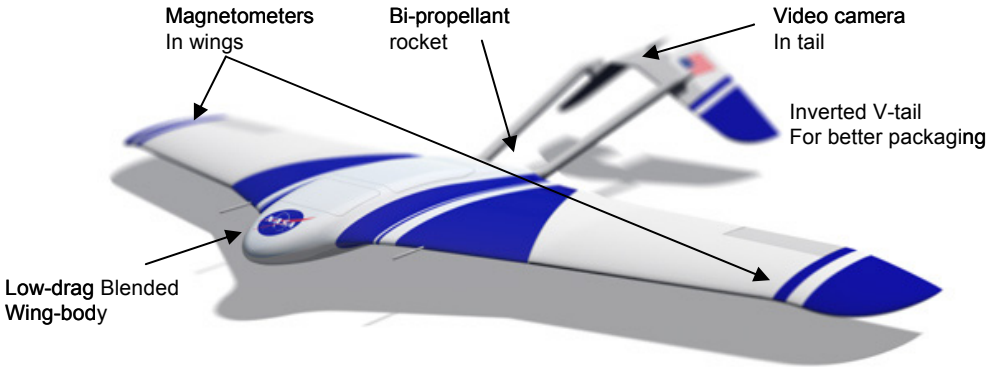

Figure 5. The ARES vehicle configuration shown with key features.

O. Model Validation

When the design variables are set at the values used in the ARES project, the subsystem masses compare favorably, but the predicted propellant load is heavier due to the slightly modified flight profile. For simplicity, the model built for this study uses a constant velocity flight profile, while the ARES team used a constant lift to drag ratio during cruise, leading to a slightly lower propellant mass. Despite these differences, the current model produces an airplane gross mass just 3.3% heavier than ARES' mass estimate. At the mission level, the life cycle cost, wet launch mass, and entry system mass are all within 9% of the ARES values. These errors are well within the accuracy of either system level model.

When optimized for endurance, the result is a vehicle capable of flying for 2.39 hrs, 79% greater endurance than ARES. This longer endurance airplane weighs 296kg, 127% more than ARES. Inclusion of the 30% launch mass margin results in the use of the same launch vehicle, the Delta II 7925. This is significantly greater endurance than found in the ARES study, but this solution does not take into account the $350 million cost cap for Discovery class missions.

P. Technology Trades

This study examines the influence of different propulsion systems and different configurations on the performance of the airplane. These are chosen because of the large dependence of the airplane endurance on the efficiency of the propulsion system, the large influence of aerodynamic performance on endurance, and the difficulty of packaging an airplane in a traditional aeroshell. Five propulsion systems and five configurations are explored. All propulsion system improvements are made from the baseline vehicle and all configuration changes are made to fit in the baseline 2.54m diameter aeroshell with a bipropellant propulsion system.

The propulsion systems explored are a NTO/MMH bipropellant rocket, a battery powered propeller, a direct methanol fuel cell powered propeller, a beamed solar powered propeller, and a beamed microwave powered propeller. The five configurations explored are a swept wing with inverted "v" tail (ARES), a straight wing with a single vertical tail, a straight wing with two vertical tails, a wing and canard, and a swept wing with two vertical tails.

IV. Modeling Techniques

The optimization problem can be stated in standard form as:

Maximize: Cruise Time
By changing: Range, Pull-up Velocity, C_3 LV
Subject to: $1-n<0$ $W_{folded}-4.8<0$
$V_{cruise}/100-1.8<0$ $Vol_{subs}-Vol_{fuse}<0$
$1.5-(gdalt/1000-D_{pullup}/1000)<0$

The objective function is to directly maximize the airplane endurance, and the design variables are the airplane range, velocity at airplane release, and the C_3 provided by the launch vehicle. In the hybrid method, the cruise velocity is optimized analytically in the performance module. This simplifies the problem for the optimizer and, since the global objective is identical to the local objective (maximum endurance), it produces a good solution.

The three design variables allow the optimizer to control the endurance of the airplane and to satisfy the constraints. By using the C_3 provided by the launch vehicle as a design variable, the optimizer is capable of making the trade between launch vehicle and spacecraft mass. The base constraints listed here set physical limits on the system. The normal force constraint is required when the optimizer is controlling the cruise velocity since maximum endurance is achieved when the velocity is minimized, possibly resulting in less lift than required to maintain level flight.

The hybrid optimization formulation was conceived after difficulty was encountered trying to implement OBD for this problem. The hybrid method uses a system level optimizer to control the design variables and FPI to converge the feedback variables, while keeping the cruise velocity optimizer in the performance contributing analysis. More on the selection of the optimization scheme can be found in Rohrschneider et al[25].

V. Results

The propulsion systems were compared over a range of scale sizes from 0.75 up to 1.75 and the configurations were compared using the biprop propulsion system in aircraft sized to fit into a 2.54m diameter aeroshell. The maximum scale size of 1.75 was chosen such that the aircraft will fit in a 5m fairing using three folds. The results of the propulsion trade are shown in Figure 6 and the configuration trade results are shown in Figure 7. All data was calculated for the 2011 launch opportunity which resulted in the C_3 being 10.53 km^2/s^2 for all cases. No results are listed for the microwave beamed power option because the resulting mission was too massive to be launched in one piece on any current or planned vehicle.

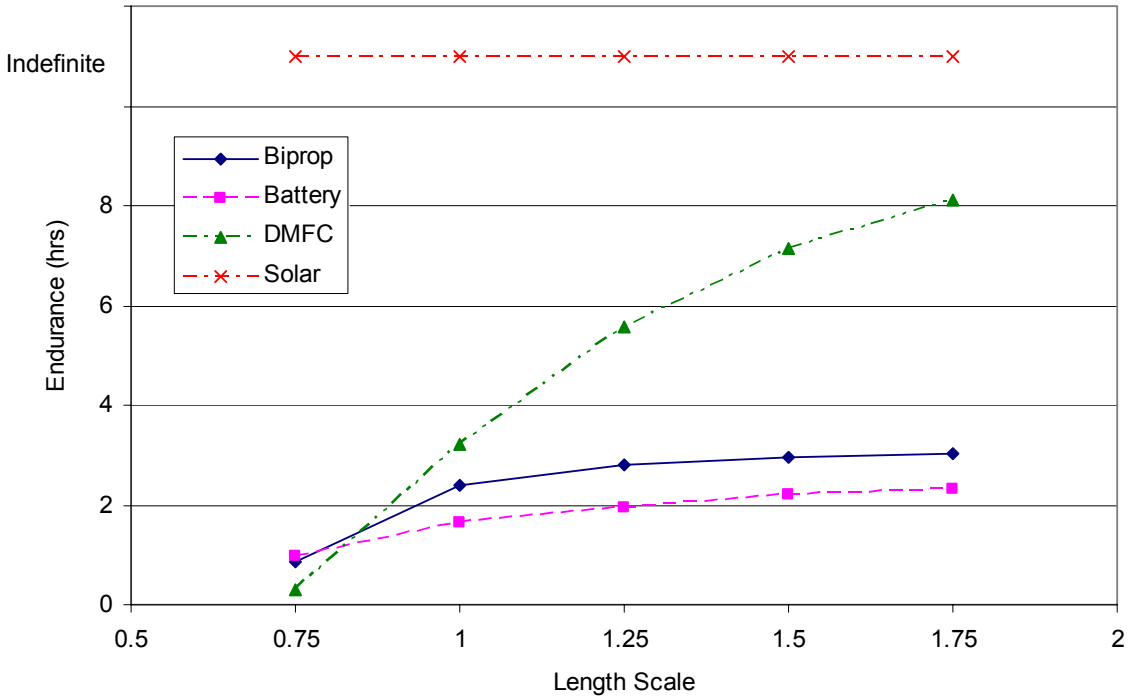

Figure 6. The airplane endurance increases with the scale size until a physical limit for that technology is reached.

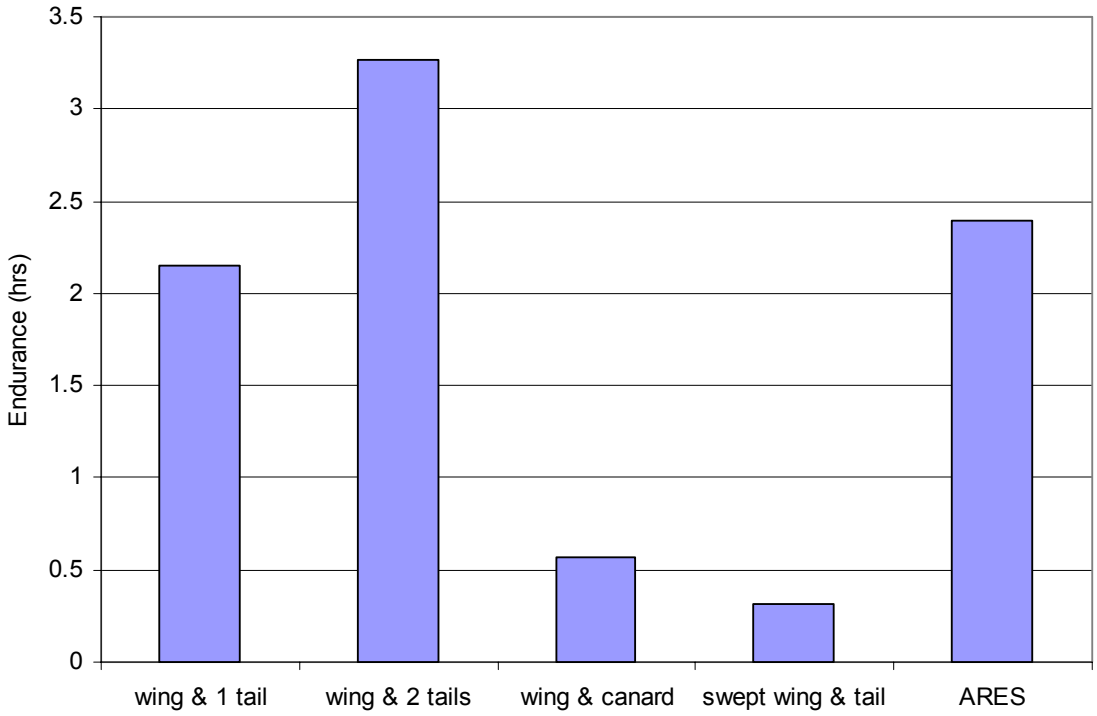

Figure 7. Each configuration has been sized to fit in a 2.54m diameter aeroshell and is powered by a biprop rocket. Differences in the endurance are largely due to the available volume in the fuselage.

These optimal solutions are constrained by their physical constraints for each technology or configuration: the useable volume, the cruise velocity, or the pull-up altitude. Table 2 lists which of the physical constraints were active for each of the optimal solutions. All of the solutions satisfied the compatibility constraints, therefore they are not included in this listing, nor is the wing loading constraint, since the analytical cruise velocity optimizer ensures that this constraint is satisfied.

Table 2. Optimal solutions were often constrained by physical limits. The different configurations were all sized to fit in a 2.54m diameter aeroshell.

Technology or Configuration	Scale Size	Constraint Active
Biprop/rocket	0.75	Volume
	1.00	Volume
	1.25	Velocity
	1.50	Velocity
	1.75	Velocity
Battery/propeller	0.75	Volume
	1.00 – 1.75	None
DMFC/propeller	0.75 – 1.75	None
Solar/propeller	0.75 – 1.75	None
Wing and single tail	0.98	Volume
Wing and double tail	0.97	Pullup
Wing and canard	0.99	Volume
Swept wing and tail	0.98	Volume

VI. Discussion

Of the five propulsion systems explored in this study, the beamed solar power system is the only feasible system to offer the potential for indefinite flight times. The DMFC powered vehicle shows significant potential for long duration flight if a better packaging method can be employed. Figure 6 shows that the endurance potential of this power system has not yet been reached, and is only limited by the payload fairing diameter available on launch vehicles. The range of each propulsion system is shown in Figure 8 and has only reached its limit for the battery powered system.

One interesting result of the analysis is that the constraints are not limiting any of the propeller driven aircraft. For smaller aircraft the rocket powered airplane is limited by the volume since the propulsion system efficiency is relatively low. For larger aircraft, velocity is the limiting factor since the mass is too high relative to the wing area. Even though the battery system has a higher energy density than the biprop system, its performance is worse since it does not lose mass throughout the flight. This results in the crossover point observed in Figure 6. At scale sizes below 1.0, the base system mass is dominant. This means that for systems like DMFC where a significant amount of hardware is required to produce any power, the endurance suffers for smaller plane sizes. The biprop system is the only one that has a near zero-intercept for the energy available vs. power system mass curve. Figure 9 shows this trend for each propulsion system. These curves are calculated for constant power output with varying flight time, depicted here as energy. The biprop system has the lowest intercept and so makes the best short endurance airplane, but is the heaviest for long endurance aircraft. The lowest curve for a given energy represents the lightest propulsion system. Care must be taken near the crossover points since the thrust efficiency of the rocket, propeller, and other systems can influence which aircraft will be the lightest.

When the mission gross mass is plotted as a function of the scale size the available launch vehicles can be overlaid and the boundaries between launch vehicles visualized. A mission planner could use this to choose the size of airplane to fly. The launch vehicle mass capability listed in Figure 10 represents the mass capability less the 30% mass margin. For the solar powered vehicle there is no dependence of mass on desired endurance, so it is purely a function of length scale. The minimum mass observed at a scale length near 1.5 does not correspond to the minimum cost mission which is observed near a scale length of 1.0. Life cycle cost data is shown in Figure 11. The only propulsion system to exhibit a minimum cost solution within the domain is the solar powered vehicle, the remainder are cheapest at the smallest scale size. The bucket in the LCC for the solar powered airplane means that it is only the cheapest option for larger vehicle scales; small vehicles favor the battery powered airplane from a cost perspective.

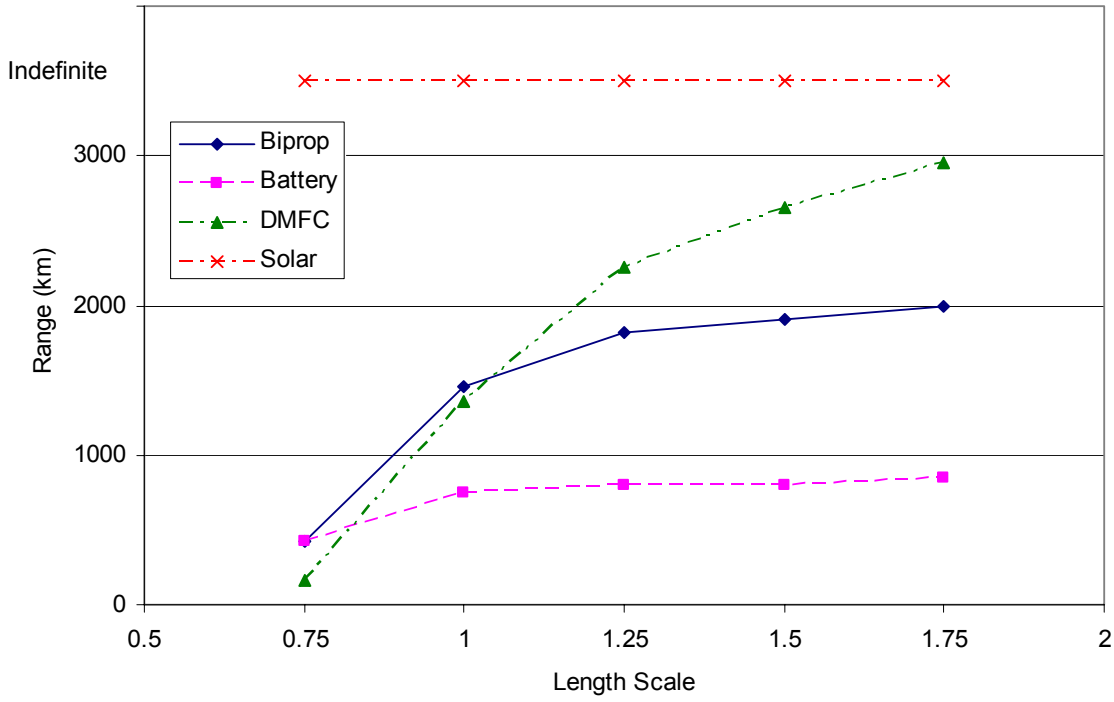

Figure 8. The range is not maximized for the vehicle, and a limit has only been reached for the battery powered airplane.

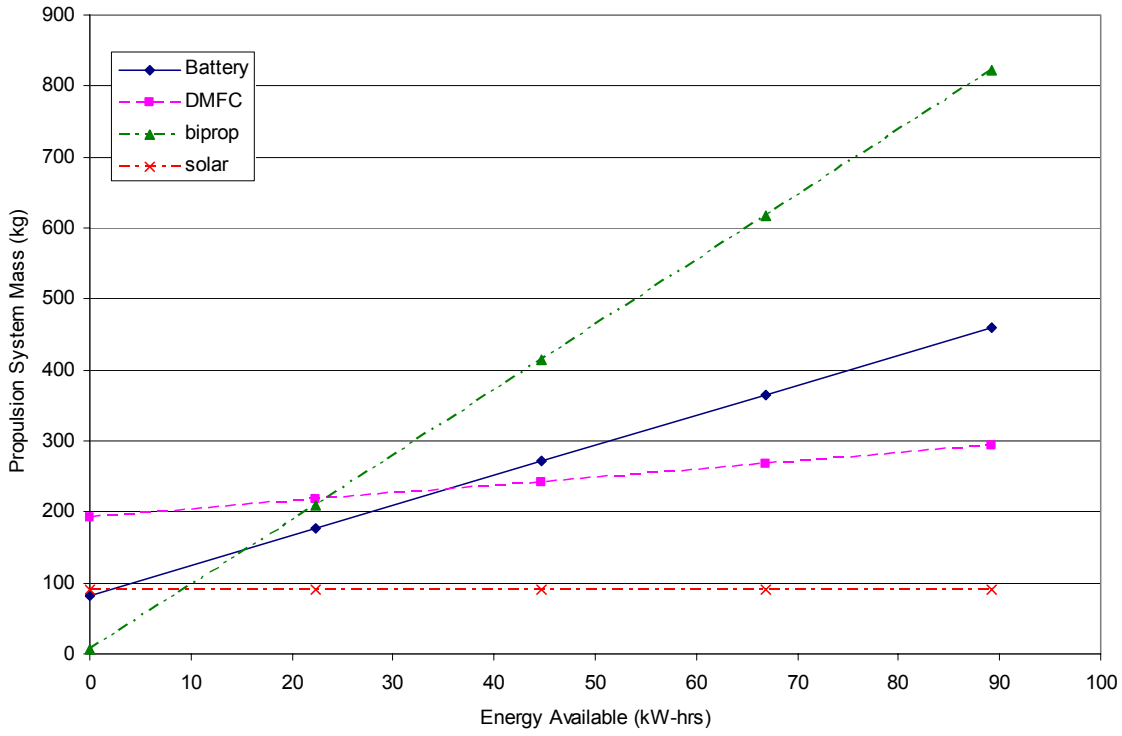

Figure 9. Propulsion system mass as a function of available energy can be used to pick the lightest propulsion system for a given flight time.

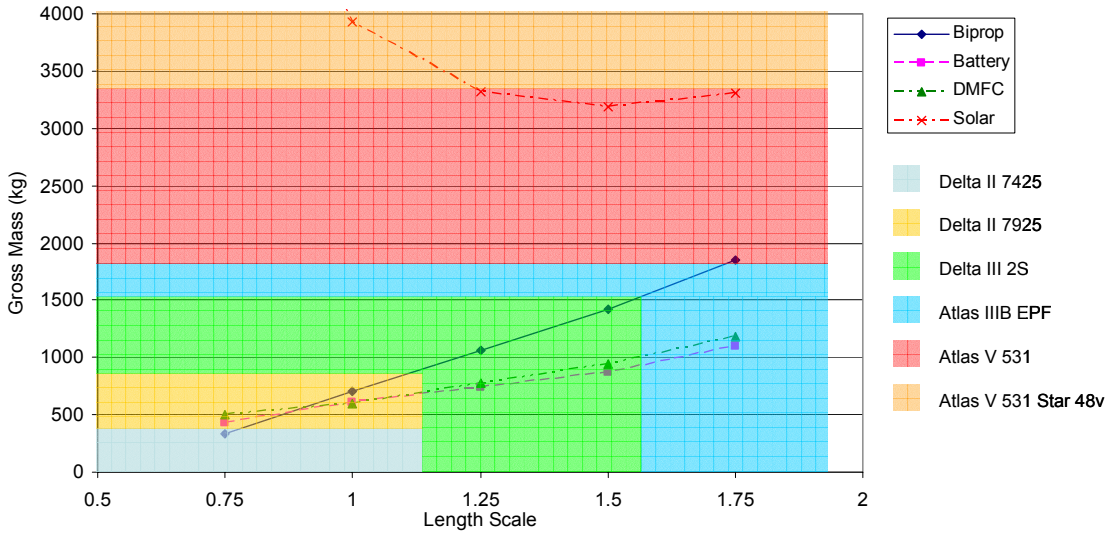

Figure 10. Launch vehicle selection for the Mars airplane can be made based on scale size and mission gross mass. Launch vehicle mass accounts for a 30% mass margin.

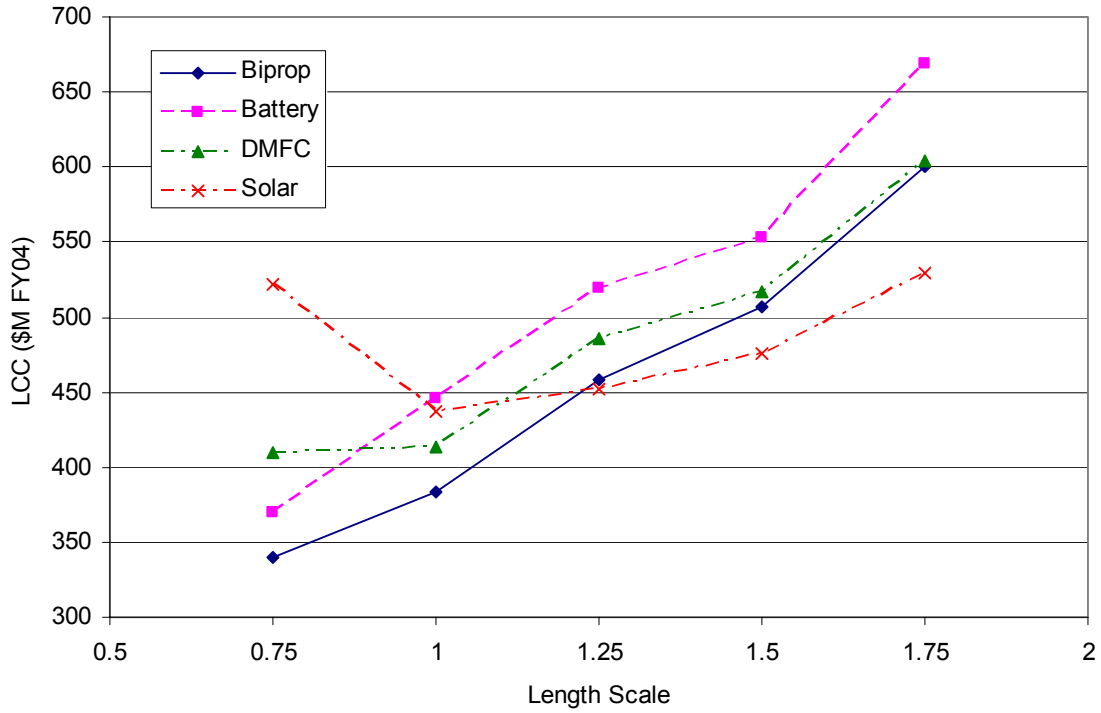

Figure 11. The lowest mission life cycle cost changes from the battery powered system to the solar powered system as the scale size increases.

The configuration trade study showed more variation in the endurance than would have been expected from the spread in aerodynamic coefficients. The low endurance observed in the wing and canard and swept wing and tail designs is due to the small fuselage being severely volume constrained. Both of these planes were scaled down considerably from their original design size to fit inside a 2.54m aeroshell, making the fuselage small compared to the wings. It is likely that the fuselage volume could be increased on these two aircraft without significant drag penalties. These were also the only two aircraft in the study that were not originally designed to be folded into an aeroshell, making them more difficult to package. The other three aircraft all had cruise times greater than 2 hours

with 3.27 hours being the best time, obtained by the wing and 2 tails design. Figure 12 shows the gross mass, cruise velocity, and LCC for each of the configurations. The wing and 2 tails design was pull-up constrained due to the higher mass of this vehicle, and hence higher ballistic coefficient of the aeroshell.

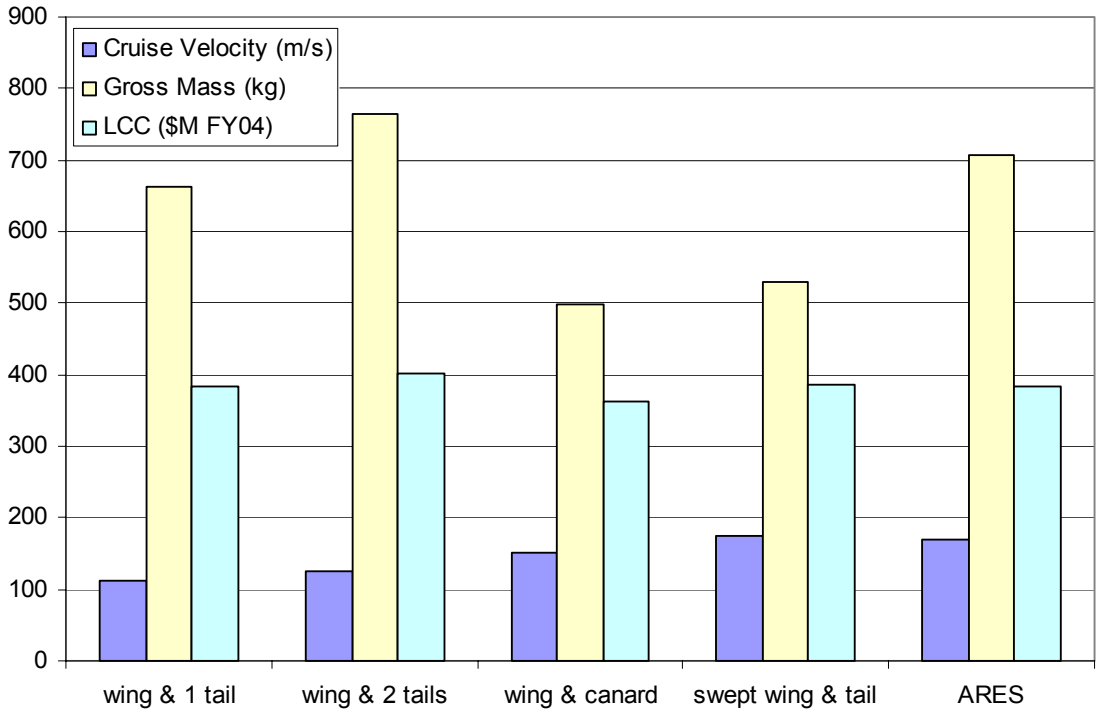

Figure 12. The longest endurance configuration also has the highest mass and is pull-up constrained.

Now that the best configuration and the best onboard power system for a long duration airplane are known, what is the endurance of the two put together? The marriage of the wing and two tails configuration to the DMFC powered propeller has an impressive endurance of 17.8 hours, a mission gross mass of 683 kg, and a life cycle cost of $407M FY04. This incredible endurance results from an airplane configuration sporting an L/D of 16.7 coupled with a very energy efficient onboard propulsion system. This configuration is pull-up constrained due to its large useable fuselage volume, which limits the endurance. A better entry method might alleviate this problem and further increase the endurance.

VII. Conclusions

The task of exploring technology and configuration options for a long duration Mars airplane was completed using the design framework ModelCenter. A hybrid optimization method was used to determine the maximum endurance aircraft for a range of scale sizes for each propulsion system. For short flight times, the bipropellant propulsion system produced the lightest vehicle. However, the DMFC powered airplane is the best onboard power system for long endurance. The beamed solar power propulsion system can potentially provide indefinite flight times if tracking accuracy can be improved on Mars. Five different configurations were studied and the wing and 2 tails design provided the longest endurance in a 2.54m diameter aeroshell. Combining the best onboard power system (DMFC) and the best configuration (wing and 2 tails) resulted in a vehicle capable of 17.8 hours of cruise costing $407M FY04, far exceeding the endurance of the baseline vehicle.

References

[1] Clarke, V.C., et al, "Final Report of the Ad Hoc Mars Airplane Science Working Group," NASA CR-158000, 1978.

[2] Cutts, J.A., et al, "Role of Mars Aerial Platforms in Future Exploration of Mars," Draft 10, August 31, 1998.

[3] Braun, R.D., Wright, H.S., Croom, M.A., Levine, J.S., and Spencer, D.A., "The Mars Airplane: A Credible Science Platform," IEEE 1260, *IEEE Aerospace Conference*, Big Sky, MT, Mar. 6-13, 2004.

[4] Levine, J.S., Blaney, D., Connemey, J., Greeley, R., Head III, J., and Hoffman, J., "Science from a Mars Airplane: The Aerial Regional-Scale Environmental Survey (ARES) of Mars," AIAA 2003-6576, *2nd AIAA "Unmanned Unlimited" Conference*, San Diego, CA, Sept. 15-19, 2003.

[5] Malone, B., Papay, M., "ModelCenter: An Integration Environment for Simulation Based Design," *Simulation Interoperability Workshop*, Orlando, FL, Mar., 1999.

[6] Humble, R.W.(ed.), Henry, G.N.(ed.), and Larsen, W.J.(ed.), *Space Propulsion Analysis and Design: Revised*, Space Technology Series, McGraw Hill Companies, Inc., New York, 1995.

[7] Hong, P.E., Kent, P.D., Olson, D.W., and Vallado, C.A., "Interplanetary Program to Optimize Simulated Trajectories (IPOST). Volume 1: Users Guide," NASA CR-189653-VOL-1-REV, 1992.

[8] Justus, C.G., and James, B.F., "Mars Global Reference Atmospheric Model 2000 Version (Mars-GRAM 2000): Users Guide," NASA TM-2000-210279, 2000.

[9] Guynn, M., Croom, M., Smith, S., Parks, R., and Gelhausen, P., "Evolution of a Mars Airplane Concept for the ARES Mars Scout Mission," AIAA 2003-6578, *2nd AIAA "Unmanned Unlimited" Conference*, San Diego, CA, Sept. 15-19, 2003.

[10] Anon, "Project Ares II: High-Altitude Battery-Powered Aircraft," *Proceedings of the Seventh Annual Summer Conference, NASA/USRA: University Advanced Design Program*, 1991, pp 29-33.

[11] Clarke, V.C., Karem, A., and Lewis, R.,"A Mars Airplane?" *Astronautics and Aeronautics*, Vol. 17, No. 1, 1979, pp 42-54.

[12] Reed, D. R., "High-Flying Mini-Sniffer RPV: Mars Bound?" *Astronautics and Aeronautics*, Vol. 16, No. 6, 1978, pp26-39.

[13] Raymer, D.P., *Aircraft Design: A Conceptual Approach*, 3rd ed., AIAA Education Series, New York, 1999.

[14] Harris, D., "Ballard Extends Industry Lead with Unveiling of Next Generation Fuel Cell," Ballard Power Systems, Inc., Burnaby, BC, Canada, January 9, 2000.

[15] Thomas, S.C., Ren, X., Gottesfeld, S., Zelanay, P., "Direct Methanol Fuel Cells: Progress in Cell Performance and Cathode Research," *Electrochimica Acta*, Vol. 47, No. 22-23, 2002, pp. 3741-3748.

[16] Ren, X., Thomas, S., Zelenay, P., and Gottesfeld, S., "Recent Advances in Direct Methanol Fuel Cells at Los Alamos National Laboratory," *Joint Fuel Cell Technology Review Conference*, Chicago, IL, Aug. 3-5, 1999.

[17] Rohrschneider, R., Sakai, T., Steffes, S., Grillmayer, G., St. Germain, B., and Olds, J., "Solar Electric Propulsion Module Concept for the *BiFrost* Architecture," IAC-02-S.4.09, *53rd International Astronautical Congress, The World Space Congress - 2002*, Houston, Texas, October 10-19, 2002.

[18] Colozza, A.J., "Preliminary Design of a Long-Endurance Mars Aircraft," NASA CR-185243, 1990.

[19] Hall, D.W., Parks, R.W., and Morris, S., "Airplane for Mars Exploration: Conceptual Design of the Full-Scale Vehicle Design, Construction and Test of Performance and Deployment Models," report submitted to NASA Ames Research Center by Dvid Hall Consulting (available at www.redpeace.org/Propulsoin.pdf).

[20] Rohrschneider, R.R., "Development of a Mass Estimating Relationship Database for Launch Vehicle Conceptual Design," Master's Special Project, Georgia Institute of Technology, Atlanta, GA, 2002.

[21] Gage, P.J., Allen Jr., G.A., Park, C., Brown, J.D., Wercinski, P.F., and Tam, T.C., "A Loaf-Shaped Entry Vehicle for a Mars Airplane (The Best Thing Since Sliced Bread?)," AIAA 2000-0634, *38th AIAA Aerospace Sciences Meeting and Exhibit*, Reno, NV, Jan 10-13, 2000.

[22] Brauer, B.L., Cornick, D.E., and Stevenson, R., "Capabilities and Applications of the Program to Optimize Simulated Trajectories," NASA CR-2770, Fegruary, 1977.

[23] Rosenberg, L., "Parametric Cost Modeling of Unmanned Space Projects When the Rules Have Just Changed," Presented at the *First Annual Joint ISPA/SCEA International Conference*, Toronto, Ontario, Canada, June 1998.

[24] Wright, H.S., Croom, M.A., Braun, R.D., Qualls, G.D. and Levine, J.S., "ARES Mission Overview – Capabilities and Requirements of the Robotic Aerial Platform," AIAA 2003-6577, *2nd AIAA "Unmanned Unlimited" Conference*, San Diego, CA, Sept. 15-19, 2003.

[25] Rohrschneider, R.R., Olds, J.R., Kuhl, C.A., Braun, R.D., Steffes, S.R., and Hutchinson Jr., V., "Modeling Approach for Analysis and Optimization of a Long-Duration Mars Airplane," 10th AIAA/ISSMO Multidisciplinary Analysis and Optimization Conference, Albany, NY, Aug 30 – Sept. 1, 2004.